ADVANCED ELECTRONIC MATERIALS
www.advelectronicmat.de

Correlating the Structural and Photophysical Properties of *Ortho*, *Meta*, and *Para*-Carboranyl–Anthracene Dyads

*Adam V. Marsh, Matthew J. Dyson, Nathan J. Cheetham, Matthew Bidwell, Mark Little, Andrew J. P. White, Colin N. Warriner, Anthony C. Swain, Iain McCulloch, Paul N. Stavrinou, Stefan C. J. Meskers, and Martin Heeney**

The role of the carborane isomer is investigated on the structural and photophysical properties of molecules comprising a carborane cluster and a conjugated organic moiety is investigated by synthesizing isomeric *o*-, *m*-, and *p*-carboranyl-anthracene donor–acceptor dyads. While appending a carborane leads to emission from a low energy intramolecular charge transfer state for the *o*-isomer, as well as emission from an excited state localized on the anthracene, this is not the case for the *m*- and *p*-carborane derivatives. This difference is attributed to a lower electron affinity for the latter two isomers. However, adding both *m*- and *p*- deforms the aromatic backbone and increases its structural rigidity, reducing non-radiative decay pathways and hence enhancing photoluminescence quantum efficiency relative to anthracene.

1. Introduction

The acenes constitute a class of molecular semiconductors with remarkable optoelectronic properties such as, for example, (electro-) luminescence, high charge carrier mobilities, and singlet fission.[1,2] Functionalization of the acene at the central carbon atoms allows further optimization of the desired properties. Here, we report the functionalization of anthracene with three different carborane isomers.

Adding a carborane cluster, with its unique icosahedral structure and σ-delocalized skeletal bonding system,[3] to a conjugated organic molecule can induce new fluorescence behaviors. Such molecules are commonly employed as fluorescent probes due to the pronounced dependence of their emission characteristics on their local environment.[4,5] Many studies focus exclusively on the widely available *o*-carborane, which has been incorporated into a range of organic fluorophores.[6–22] When attached to an aryl donor group, the carborane can accept an electron upon photoexcitation of the aryl-carborane molecule through photoinduced intramolecular charge transfer (ICT). The orbital overlap required for charge transfer results from extension of the π-system of the anthracene donor onto the antibonding orbital of the carboranyl carbon-carbon (C_C–C_C) bond.[8,15–18,23–25] This orbital overlap depends on the molecular geometry and is expected to be largest with a perpendicular arrangement of the C_C–C_C bond relative to the plane of the donor π-system. The charge transfer coupled to rearrangement of the internal molecular geometry allows for a twisted-ICT (TICT) state.[25–38] Emission from such a molecular geometry depends strongly on the environment;[5,39–44] in good solvents these states are mostly non-emissive due to non-radiative decay through vibration of the flexible C_C–C_C bond, but this emission can be recovered in a sterically

Dr. A. V. Marsh, M. Bidwell, Dr. M. Little, Dr. A. J. P. White, Prof. M. Heeney
Department of Chemistry and Centre for Plastic Electronics
Imperial College London
South Kensington
London SW7 2AZ, UK
E-mail: m.heeney@imperial.ac.uk

Dr. M. J. Dyson, Prof. S. C. J. Meskers
Molecular Materials and Nanosystems and
Institute for Complex Molecular Systems
Eindhoven University of Technology
Eindhoven, MB 5600, The Netherlands

The ORCID identification number(s) for the author(s) of this article can be found under https://doi.org/10.1002/aelm.202000312.

DOI: 10.1002/aelm.202000312

Dr. N. J. Cheetham
Department of Physics and Centre for Plastic Electronics
Imperial College London
South Kensington
London SW7 2AZ, UK

Dr. C. N. Warriner, Dr. A. C. Swain
AWE, Aldermaston
Reading RG7 4PR, UK

Prof. I. McCulloch
King Abdullah University of Science and Technology (KAUST)
KAUST Solar Center (KSC)
Division of Physical Sciences and Engineering
Thuwal 23955-6900, Saudi Arabia

Prof. P. N. Stavrinou
Department of Engineering Science
University of Oxford
Oxford OX1 3PJ, UK

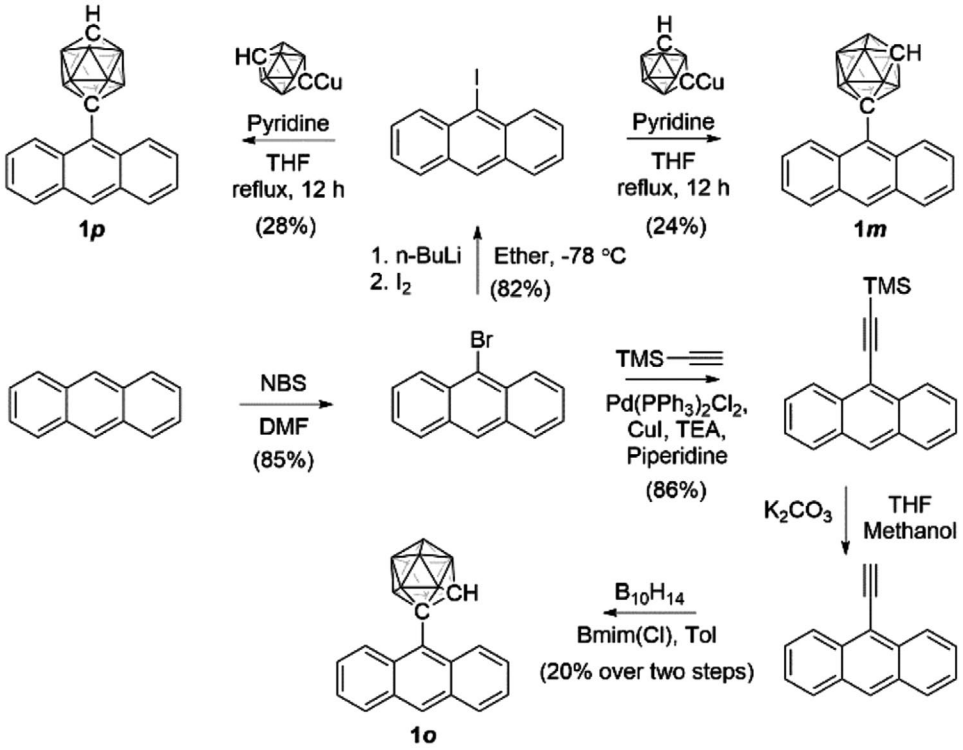

Scheme 1. The synthesis of **1*o***, **1*m***, and **1*p***.

restricted environment; most notably when the molecules are aggregated, leading to aggregation-induced emission (AIE).[39–74]

In contrast, *m*- and *p*-carborane isomers are far less investigated; however, there are some reports of their incorporation into organic fluorophores. *m*-Carborane has been used in π-conjugated polymers to aid stability and polymerization,[71,75] and in small molecules to increase fluorescence by sterically blocking intermolecular π-stacking interactions.[76] Furthermore, both *m*- and *p*-isomers have been incorporated into molecular fluorophores without adversely affecting emission intensity,[77] and radical anions of *p*-carborane bonded to phenylene groups reportedly display efficient charge transfer.[78] One report also demonstrates that *m*- and *p*-carborane can dramatically enhance the emission of triphenylbenzene trimers.[79] Inspired by these results, we set out to gain a fundamental understanding of the photophysics of all three carboranyl isomers, using a model system of an anthracene–carborane donor–acceptor dyad. In particular, we aim to establish how and why the characteristics previously observed for *o*-carborane derivatives, depend on the choice of isomer.

2. Results and Discussion

We begin by considering the three icosahedral carborane isomers, which are distinguished by the relative position of the two carbon atoms in the boron cage. Specifically, the *o*-, *m*-, and *p*-carborane isomers have carbon atoms in the 1,2, 1,7, and 1,12 cage positions, respectively. The three parent carborane isomers exhibit remarkable thermal and chemical stability and are known to confer these properties onto compounds to which they are substituted.[3] Thermal stability increases on the order $o < m < p$, allowing for the synthesis of *m*- and *p*-carboranes from thermal isomerization of *o*-carborane[80] (itself synthesized from a reaction of decaborane with acetylene).[81] All carborane isomers are electron-withdrawing units when substituted at the carbon atom, but *m*- and *p*-carboranes are significantly less electron withdrawing than the *o*-isomer, owing to the more uniform distribution of electron density as the carboranyl carbon atoms are more spatially separated.[3]

The anthracene–carbonyl dyads are synthesized, as shown in **Scheme 1** to afford 1-(9′-anthracenyl)-*o*-$C_2B_{10}H_{11}$ (**1*o***), 1-(9′-anthracenyl)-*m*-$C_2B_{10}H_{11}$ (**1*m***), and 1-(9′-anthracenyl)-*p*-$C_2B_{10}H_{11}$ (**1*p***). **1*o*** was synthesized via ionic-liquid catalyzed[82–84] decaborane/alkyne coupling via 9-ethynylanthracene, in a slight yield improvement on a literature procedure (20% and 18%, respectively).[26] Novel compounds **1*m*** and **1*p*** were prepared via reaction of the carboranyl cuprates with 9-iodoanthracene in the presence of pyridine.[85] Yields for these reactions (24% and 28% for **1*m*** and **1*p***, respectively) are relatively low, reflecting the difficulty in introducing bulky carboranes to the sterically crowded environment around the 9-position of anthracene.

Single crystals of the three products were grown by slow evaporation from a biphasic solution of dichloromethane (DCM) and hexane and subjected to X-ray diffraction analysis. Crystal structures and selected aromatic deformation parameters are presented in **Figure 1** and **Table 1**, respectively, with detailed crystallography data presented in Figures S13–S19, Supporting Information.

Each anthracene–carborane isomer exhibits significant deformation of the aromatic ring system as a result of carborane incorporation, but there is notable variation between the

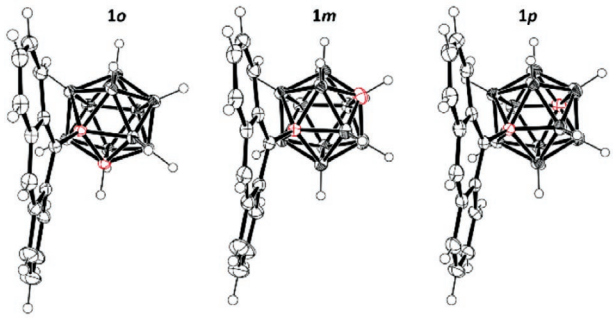

Figure 1. ORTEP[93] representations of the crystal structures of **1*o***, **1*m***, and **1*p***. Carboranyl carbon atoms are depicted in red for clarity. Ellipsoids drawn at 50% probability.

compounds. The deformation angles α and β, as defined in Figure S13, Supporting Information, differ between the isomers, with their sum increasing on the order **1*p*** < **1*m*** < **1*o***. Similarly, ϕ, the deviation from an ideal 180° axis of rotation is distinctly larger for **1*o***. While all three carboranyl isomers are icosahedral, there are important differences in their structure; *p*-carborane is the most symmetrical and least bulky substituent, whereas *o*-carborane is the least symmetrical and most bulky. The C_C–C_C bond of **1*o*** is proximal to, and approximately co-planar with, the anthracene moiety, and is shorter than the C–B bonds observed in the same position for **1*m*** and **1*p*** (1.664, 1.741, and 1.744 Å, respectively). Thus, the C–H vertex of *o*-carborane projects towards the anthracene moiety at a more acute angle than the equivalent B–H vertices in **1*m*** and **1*p***. Larger steric interactions result, leading to greater structural deformation of the anthracenyl moiety to accommodate *o*-carborane.

To investigate the impact of carborane isomer on structural rigidity, which influences the photoluminescence (PL) quantum yield (PLQY, Φ), we undertook a temperature-dependent ^{1}H NMR study focusing on the anthracenyl C(1) and C(8) proton resonances, which are proximal to the carborane cages.

Figure 2a shows that upon cooling, there are no significant changes to the peak width and position of the **1*p*** NMR spectrum. For **1*m*** however, there is a distinct broadening of the anthracenyl C(1)-H and C(8)-H proton resonances as the temperature is reduced, and for **1*o*** a similar degree of broadening was observed at room temperature. When **1*o*** is cooled the C(1)-H and C(8)-H peaks separate and are distinguishable in the NMR spectrum. These phenomena can be explained by carboranyl rotational degrees of freedom; a density functional theory (DFT) computational study analyzing the change in potential energy of the synthesized compounds as a function of carborane rotation angle relative to the plane of anthracene is presented in Figure 2b, with computational details outlined in the Supporting Information.

1*p* has five-fold rotational symmetry, indicative of a single ground state geometry, whereas both **1*m*** and **1*o*** display more

Table 1. Aromatic deformation parameters for **1*o***, **1*m***, and **1*p***.

Isomer	α [°]	β [°]	α + β [°]	ϕ [°]
1*o*	13.39	7.28	20.67	7.87
1*m*	14.89	5.65	20.54	4.32
1*p*	13.33	5.62	18.95	3.10

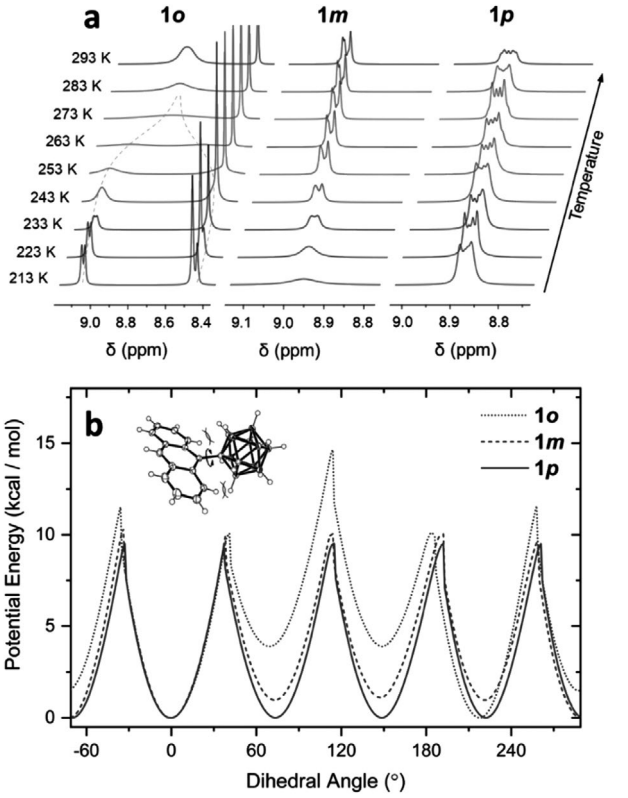

Figure 2. a) Temperature-dependent ^{1}H NMR ($CDCl_3$) of the anthracenyl C(1) and C(8) protons of **1*o***, **1*m***, and **1*p***, concentration = 1×10^{-4} M. b) DFT (B3LYP/6-31G(d); gas phase) calculated, normalized potential energy surface (PES) of **1*o***, **1*m***, and **1*p***, as a function of the dihedral angle between the carborane and anthracene, at 1° resolution, with a depiction of the steric interactions for **1*o*** between the carborane and the anthracenyl C(1)-H and C(8)-H vertices. The arbitrarily assigned 0° angle is the ground state geometry, with potential energy minima geometries for all isomers presented in Figure S20, Supporting Information.

variability in potential energy across the 360° of rotation. These both feature three different low energy conformations in the ground state, reflecting the symmetries of the parent carboranes. The largest potential energy barrier to rotation increases in the order **1*p*** < **1*m*** < **1*o*** (9.52, 10.31, and 14.63 kcal mol^{-1}, respectively), which is consistent with the trends in deformation parameters gained from the crystallographic studies. **1*p***, therefore, with its rotational symmetry about the central donor-acceptor bond, has the lowest barrier to carborane rotation of the three isomers. Accordingly, even at low temperatures there is sufficient kinetic energy in the system such that carborane rotation is fast with respect to the chemical shift difference between the C(1)-H and C(8)-H peaks at the NMR fields used in these experiments. In contrast, **1*m*** has a larger barrier to rotation; at lower temperatures carborane rotation is thus somewhat restricted, leading to the proximal anthracenyl protons experiencing a broad distribution of electronic environments depending on the relative orientation of the carborane. The same is true for **1*o*** at room temperature, but cooling severely restricts carborane rotation such that C(1)-H and C(8)-H protons become inequivalent, and two peaks can be observed in the spectrum. Further cooling essentially freezes the carborane on the

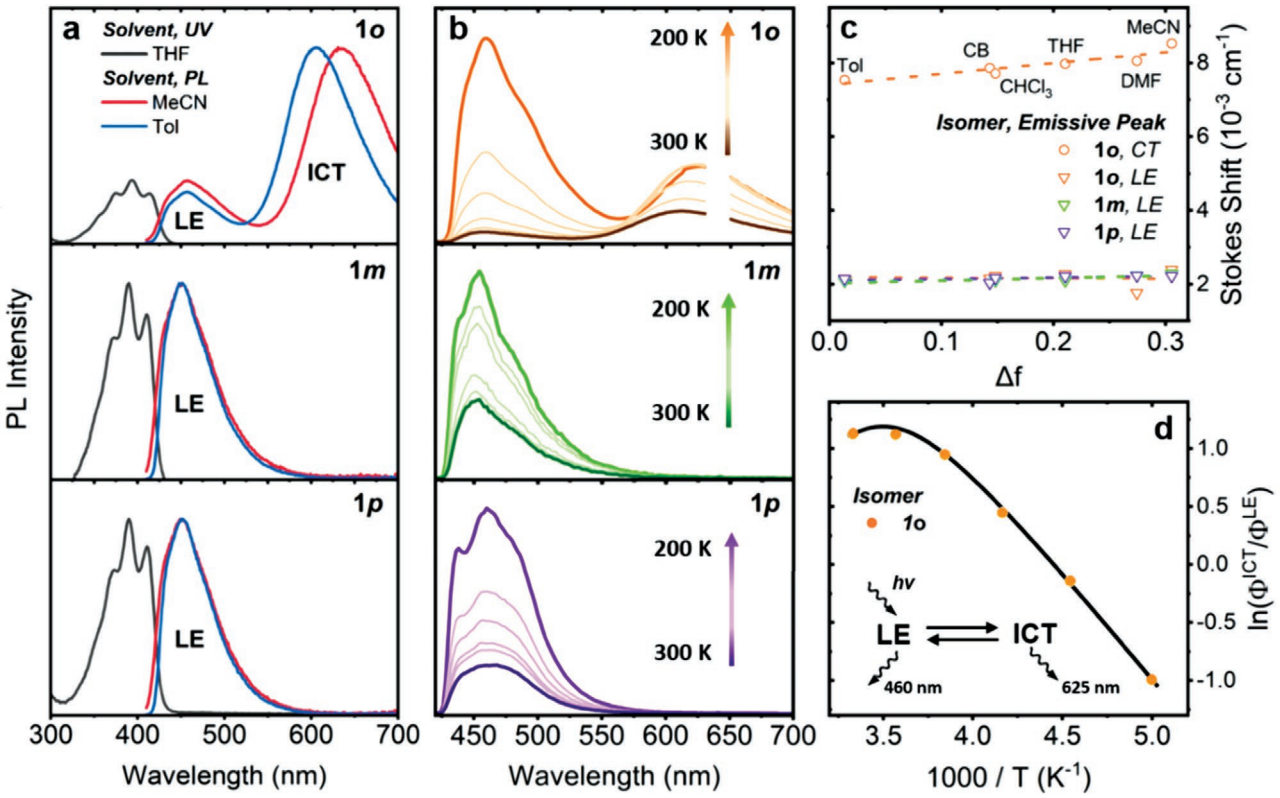

Figure 3. a) Normalized UV (in THF) and PL emission spectra (in MeCN and Tol), λ_{ex} = 400 nm of **1*o***, **1*m***, and **1*p***. b) Temperature-dependent PL of **1*o***, **1*m***, and **1*p*** in $CHCl_3$, λ_{ex} = 320 nm. c) Lippert–Mataga plot with linear fitting, and d) Stevens–Ban plot of **1*o***. Concentration = 1×10^{-4} M.

NMR timescale, recovering the J-coupling fine structure for the distinguishable C(1)-H and C(8)-H peaks. From these NMR and computational studies, it was concluded that steric interactions between the carborane and anthracene moieties and, following this, structural rigidity, increases on the order **1*p*** < **1*m*** < **1*o***. The structural rigidity of *o*-carboranyl–acene dyads has been shown to impact their optical properties significantly; the increase in Φ observed upon aggregation of these compounds (AIE) is attributed to the reduction of non-radiative decay pathways associated with molecular vibration and rotation.[39–48] Therefore, to investigate the effects of the observed divergences in structural rigidity between the isomers on their optical properties, we undertook a solvatochromic PL study (**Figure 3**a), and a temperature-dependent PL investigation of the three isomers in $CHCl_3$, using the same solution concentration as in the temperature-dependent NMR study, (Figure 3b). Steady-state UV, and PL plots for all solvents used in the solvatochromic study can be found in Figures S21–S23, Supporting Information.

Figure 3a demonstrates a similarity in the PL behavior between the carborane-anthracene isomers; all exhibit a high energy emission peak with vibronic structure that mirrors their absorbance spectra. Using a Lippert–Mataga plot (Figure 3c), shows that the high energy emission for all isomers has a Stokes shift that is independent of the solvent orientation polarizability, Δ*f*, and it is also independent of concentration (Figure S22, Supporting Information). This is indicative of local emission (LE), which originates from the anthracene moiety. Furthermore, Figure 3b shows that the intensity of these LE peaks increases inversely with temperature, but that λ_{max} is independent of temperature. As shown in Figure 2, at reduced temperatures, the **1*m*** and **1*o*** isomers show restricted carborane rotation, with the independence of the λ_{max} with temperature suggesting the LE is also independent of carboranyl dihedral geometry. Notably, however, the high energy PL emission for all isomers is red-shifted relative to the LE of pure anthracene (λ_{max} = 358 nm in cyclohexane),[49] and the peak for **1*o*** is red-shifted further relative to **1*m*** and **1*p*** (λ_{max} = 460 vs 450 nm, respectively). Clearly therefore, while these studies indicate that the LE for the three isomers originates in the anthracene moiety, it is likely that there is some inductive contribution from the carboranes. This is exacerbated in the case of **1*o*** due to the highly electron-withdrawing *o*-carborane, which is also independent of carborane dihedral geometry.

Unlike the other isomers, **1*o*** exhibits a second, low energy emissive band which is both solvent and temperature dependent. The solvatochromic shift of the low energy emission (see the Lippert–Mataga plot in Figure 3c) indicates a substantial change in the electric dipole moment in the excited state relative to the ground state and is consistent with the proposed ICT character of the relaxed, emissive excited state. Moreover, the LE and ICT states are related. Figure 3d shows a Stevens-Ban plot,[86] where $\ln(\Phi^{ICT}/\Phi^{LE})$ plotted against reciprocal temperature follows a shape characteristic of the low-temperature limit of a LE/ICT reaction; at low temperature LE dominates, and at high temperature ICT emission dominates. For **1*o***, the increase in temperature likely provides the activation energy for

the carborane to rotate away from the ground state geometry, where the C_C–C_C bond is coplanar with anthracene, to where the C_C–C_C is twisted (i.e., approximately perpendicular to anthracene), in a geometry known to facilitate charge-transfer. Similar observations have been made elsewhere,[26] and accordingly the high and low energy emissions from **1*o*** are assigned as LE and TICT states, respectively.

Notably, no such TICT or other ICT emission peak is present in the spectra of **1*m*** and **1*p***. For *o*-carborane, such species are known to be promoted when environmental factors restrict motion. Therefore, to investigate the effect of restricted motion on the PL of the three isomers, water (a poor solvent for these carborane-anthracene isomers) was incrementally added to THF solutions of all isomers to promote aggregation. We then investigated the PL of varying proportions of H_2O/THF (v/v) solvents and solid (polycrystalline) state emission. These spectra are presented in **Figure 4**, with PL quantum yield data in **Table 2**.

For **1*o*** in THF solution, adding water increases the intensity of the long-wavelength emission band, however at 50/50 v/v the PL spectrum is dominated by a broad emission at λ_{max} = 550 nm, not seen in the earlier PL studies. We hypothesize that this emissive peak may result from the mixing of LE and ICT wavefunctions,[87] promoted by a moderately polar solvent which neither favors unpolarized (i.e., LE) states nor strongly polarized states (i.e., ICT). Mixing of these states has been observed elsewhere for *o*-carboranyl derivatives when the C_C–C_C bond was coplanar with the substituent.[17] We postulate, that **1*o*** can be considered to follow the planar-ICT (PICT) model, where 90° twisting of the C_C–C_C bond relative to the anthracene moiety is not always necessary for an efficient ICT reaction, and that emission from a coplanar ICT state is possible in moderately polar solutions.[88]

At higher H_2O proportions (>80/20 v/v) the TICT emission returns with a dramatic increase in Φ. The PL efficiency of the lower energy TICT emission is also concentration-dependent, increasing with concentration, suggesting it is due to aggregation (Figure S25, Supporting Information). These data match many previous reports of a dramatic increase in PL efficiency upon aggregation, that is, AIE.[39–74]

The PLQYs of **1*m*** and **1*p*** in THF solution are remarkably high, notably higher than the parent anthracene in similar environments (Φ = 0.23, 0.27, and 0.27 in cyclohexane, ethanol, and benzene, respectively).[89,90] This is likely a result of the molecular rigidity introduced by the carboranes, reducing vibration and acting as bulky groups blocking π–π stacking of the anthracene units, associated with non-radiative decay.[79] Increasing H_2O proportions for both **1*m*** and **1*p*** solutions leads to poorly emissive solutions, likely a result of water quenching singlet excited states in lower H_2O concentrations,[91] and aggregation caused quenching in larger H_2O proportions. Interestingly, however, at 99/1 v/v solvent proportions and in the solid state for both compounds, the LE is replaced by new, red-shifted emissive peaks. The spectral shapes of these lack the vibronic character of the LE, and the PL efficiency is drastically reduced. In addition, while visually similar, the λ_{max} distinctly varies between **1*m*** and **1*p***. Polycyclic aromatic compounds such as anthracene are well known to form excimers in aggregated states, and the interactions of the π-systems can lead to non-radiative decay of excited states. The exact emission wavelength of anthracenyl excimers is also strongly dependent on the packing structure.[92] It is possible that these new emissive states are in fact weakly emissive excimers, formed from π-overlap of anthracene moieties in the aggregated states, which act predominantly as quenchers of the LE.

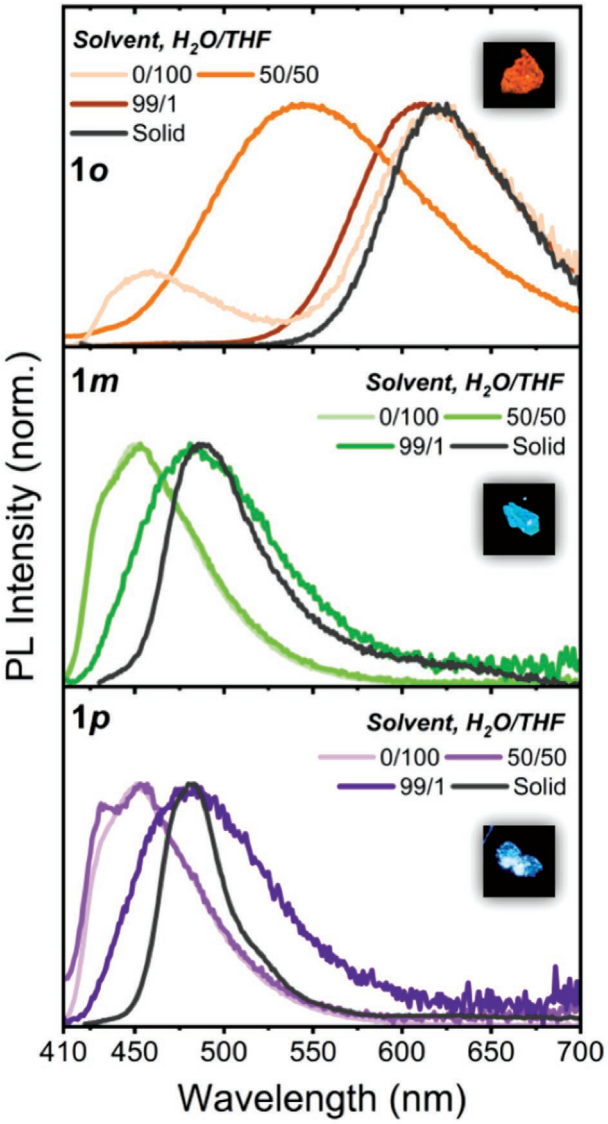

Figure 4. PL spectra of **1*o***, **1*m***, and **1*p*** in varying proportions of H_2O/THF v/v solvents and in the solid state (λ_{ex} = 400 nm), accompanied by photographs of their crystals under UV irradiation (λ_{ex} = 365 nm). Solution concentration = 1×10^{-5} M.

The lack of ICT emission from both **1*m*** and **1*p*** isomers from these PL studies is in stark contrast to the complex ICT behavior observed from **1*o***. It appears that *m*- and *p*-carboranes are, for all dihedral geometries, too weakly electron-withdrawing to facilitate charge transfer from aryl groups, at least in the neutral state. They do, however, show great promise as enhancers of the emission intensity of aromatic fluorophores in good solvents.

Table 2. Peak emission wavelengths and PL quantum yields of **1*o***, **1*m***, and **1*p*** in a THF solution, H_2O/THF v/v 99/1 aggregated solution, and in the solid state.

	Sample	λ_{max} [nm]	Φ; λ_{ex} [nm]
1*o*	THF	458, 620	0.02;[a] 375
	H_2O/THF, 99/1	611	0.18; 350
	Solid	620	0.38;[a] 375
1*m*	THF	450	0.85; 412
	H_2O/THF, 99/1	486	0.11; 412
	Solid	488	0.08; 412
1*p*	THF	450	0.70; 412
	H_2O/THF, 99/1	483	0.09; 412
	Solid	482	0.31; 412

[a]Data as reported in literature.[26]

3. Conclusions

To conclude, isomeric *o*-, *m*-, and *p*-carboranyl–anthracene dyads were synthesized. Aromatic deformation increased on the order $p < m < o$ isomers, coinciding with increased structural rigidity and a slowing of carboranyl rotation. For *m*- and *p*-isomers, the reduction of vibrational and rotational decay pathways led to significant increases in the quantum efficiency of the high energy LE when compared to the parent anthracene, showing the potential of *m*- and *p*-carboranes as PL efficiency enhancing functional groups for photoluminescent materials. Most notably, while the *o*-isomer exhibited both a LE and a low-energy TICT state, the latter was not present for *m*- and *p*-isomers and attributed to an insufficient energetic offset between anthracene and the less electron-withdrawing *m*- and *p*-carboranes.

Supporting Information

Supporting Information is available from the Wiley Online Library or from the author.

Acknowledgements

The authors thank the EPRSC for funding (EP/G037515/1 & EP/L016702/1) and AWE for their input and financial support of A.V.M. The authors also thank the Marie Skłodowska-Curie Actions Innovative Training Networks "H2020-MSCA-ITN-2014 INFORM-675867" for funding.

Conflict of Interest

The authors declare no conflict of interest.

Keywords

carborane, organic optoelectronics, organic semiconductors

Received: March 24, 2020
Published online: June 23, 2020

[1] J. E. Anthony, *Chem. Rev.* **2006**, *106*, 5028.
[2] J. Guo, D. Liu, J. Zhang, J. Zhang, Q. Miao, Z. Xie, *Chem. Commun.* **2015**, *51*, 12004.
[3] R. N. Grimes, *Carboranes*, Academic Press, Boston, MA **2016**.
[4] A. Wu, J. L. Kolanowski, B. B. Boumelhem, K. Yang, R. Lee, A. Kaur, S. T. Fraser, E. J. New, L. M. Rendina, *Chem. - Asian J.* **2017**, *12*, 1704.
[5] J. J. Peterson, A. R. Davis, M. Werre, E. B. Coughlin, K. R. Carter, *ACS Appl. Mater. Interfaces* **2011**, *3*, 1796.
[6] Y. Morisaki, M. Tominaga, T. Ochiai, Y. Chujo, *Chem. - Asian J.* **2014**, *9*, 1247.
[7] T. Kim, H. Kim, K. M. Lee, Y. S. Lee, M. H. Lee, *Inorg. Chem.* **2013**, *52*, 160.
[8] D. Tu, P. Leong, S. Guo, H. Yan, C. Lu, Q. Zhao, *Angew. Chem., Int. Ed.* **2017**, *56*, 11370.
[9] K. Nishino, K. Hashimoto, K. Tanaka, Y. Morisaki, Y. Chujo, *Sci. China: Chem.* **2018**, *61*, 940.
[10] Z. Wang, P. Jiang, T. Wang, G. J. Moxey, M. P. Cifuentes, C. Zhang, M. G. Humphrey, *Phys. Chem. Chem. Phys.* **2016**, *18*, 15719.
[11] A. Ferrer-Ugalde, A. González-Campo, C. Viñas, J. Rodríguez-Romero, R. Santillan, N. Farfán, R. Sillanpää, A. Sousa-Pedrares, R. Núñez, F. Teixidor, *Chem. - Eur. J.* **2014**, *20*, 9940.
[12] M. Tominaga, Y. Morisaki, Y. Chujo, *Macromol. Rapid Commun.* **2013**, *34*, 1357.
[13] M. Eo, M. H. Park, T. Kim, Y. Do, M. H. Lee, *Polymer* **2013**, *54*, 6321.
[14] L. Böhling, A. Brockhinke, J. Kahlert, L. Weber, R. A. Harder, D. S. Yufit, J. A. K. Howard, J. A. H. MacBride, M. A. Fox, *Eur. J. Inorg. Chem.* **2016**, *2016*, 403.
[15] L. Weber, J. Kahlert, R. Brockhinke, L. Böhling, J. Halama, A. Brockhinke, H.-G. Stammler, B. Neumann, C. Nervi, R. A. Harder, M. A. Fox, *Dalton Trans.* **2013**, *42*, 10982.
[16] S. Kwon, K.-R. Wee, Y.-J. Cho, S. O. Kang, *Chem. - Eur. J.* **2014**, *20*, 5953.
[17] L. Weber, J. Kahlert, R. Brockhinke, L. Böhling, A. Brockhinke, H.-G. Stammler, B. Neumann, R. A. Harder, M. A. Fox, *Chem. - Eur. J.* **2012**, *18*, 8347.
[18] J. Kahlert, L. Böhling, A. Brockhinke, H.-G. Stammler, B. Neumann, L. M. Rendina, P. J. Low, L. Weber, M. A. Fox, *Dalton Trans.* **2015**, *44*, 9766.
[19] S.-Y. Kim, A.-R. Lee, G. F. Jin, Y.-J. Cho, H.-J. Son, W.-S. Han, S. O. Kang, *J. Org. Chem.* **2015**, *80*, 4573.
[20] A. Ferrer Ugalde, E. J. Juárez-Pérez, F. Teixidor, C. Viñas, R. Sillanpää, E. Pérez-Inestrosa, R. Núñez, *Chem. - Eur. J.* **2012**, *18*, 544.
[21] I. Nar, A. Atsay, A. Buyruk, H. P. Karaoğlu, A. Kalkan Burat, E. Hamuryudan, *New J. Chem.* **2019**, *43*, 4471.
[22] K. Nishino, Y. Morisaki, K. Tanaka, Y. Chujo, *New J. Chem.* **2017**, *41*, 10550.
[23] L. Weber, J. Kahlert, L. Böhling, A. Brockhinke, H.-G. Stammler, B. Neumann, R. A. Harder, P. J. Low, M. A. Fox, *Dalton Trans.* **2013**, *42*, 2266.
[24] K.-R. Wee, W.-S. Han, D. W. Cho, S. Kwon, C. Pac, S. O. Kang, *Angew. Chem., Int. Ed.* **2012**, *51*, 2677.
[25] X. Wu, J. Guo, W. Jia, J. Zhao, D. Jia, H. Shan, *Dyes Pigm.* **2019**, *162*, 855.
[26] H. Naito, K. Nishino, Y. Morisaki, K. Tanaka, Y. Chujo, *Angew. Chem., Int. Ed.* **2017**, *56*, 254.
[27] S.-Y. Kim, Y.-J. Cho, G. Fan Jin, W.-S. Han, H.-J. Son, D. Won Cho, S. Ook Kang, *Phys. Chem. Chem. Phys.* **2015**, *17*, 15679.
[28] X. Wu, J. Guo, J. Zhao, Y. Che, D. Jia, Y. Chen, *Dyes Pigm.* **2018**, *154*, 44.

[29] H. Mori, K. Nishino, K. Wada, Y. Morisaki, K. Tanaka, Y. Chujo, *Mater. Chem. Front.* **2018**, *2*, 573.
[30] K. Nishino, K. Uemura, M. Gon, K. Tanaka, Y. Chujo, *Molecules* **2017**, *22*, 2009.
[31] H. Naito, K. Nishino, Y. Morisaki, K. Tanaka, Y. Chujo, *J. Mater. Chem. C* **2017**, *5*, 10047.
[32] K. Nishino, H. Yamamoto, K. Tanaka, Y. Chujo, *Org. Lett.* **2016**, *18*, 4064.
[33] J. Li, C. Yang, X. Peng, Y. Chen, Q. Qi, X. Luo, W.-Y. Lai, W. Huang, *J. Mater. Chem. C* **2018**, *6*, 19.
[34] Y. Wan, J. Li, X. Peng, C. Huang, Q. Qi, W.-Y. Lai, W. Huang, *RSC Adv.* **2017**, *7*, 35543.
[35] M. Rang Son, Y.-J. Cho, S.-Y. Kim, H.-J. Son, D. Won Cho, S. Ook Kang, *Phys. Chem. Chem. Phys.* **2017**, *19*, 24485.
[36] X. Wu, J. Guo, Y. Quan, W. Jia, D. Jia, Y. Chen, Z. Xie, *J. Mater. Chem. C* **2018**, *6*, 4140.
[37] K. Nishino, H. Yamamoto, K. Tanaka, Y. Chujo, *Asian J. Org. Chem.* **2017**, *6*, 1818.
[38] X. Wu, J. Guo, Y. Cao, J. Zhao, W. Jia, Y. Chen, D. Jia, *Chem. Sci.* **2018**, *9*, 5270.
[39] A. V. Marsh, N. J. Cheetham, M. Little, M. Dyson, A. J. P. White, P. Beavis, C. N. Warriner, A. C. Swain, P. N. Stavrinou, M. Heeney, *Angew. Chem., Int. Ed.* **2018**, *57*, 10640.
[40] B. H. Choi, J. H. Lee, H. Hwang, K. M. Lee, M. H. Park, *Organometallics* **2016**, *35*, 1771.
[41] Z. Wang, T. Wang, C. Zhang, M. G. Humphrey, *ChemPhotoChem* **2018**, *2*, 369.
[42] H. Naito, Y. Morisaki, Y. Chujo, *Angew. Chem., Int. Ed.* **2015**, *54*, 5084.
[43] Y. Nie, H. Zhang, J. Miao, X. Zhao, Y. Li, G. Sun, *J. Organomet. Chem.* **2018**, *865*, 200.
[44] Y. Chen, J. Guo, X. Wu, D. Jia, F. Tong, *Dyes Pigm.* **2018**, *148*, 180.
[45] Y. Hong, J. W. Y. Lam, B. Z. Tang, *Chem. Soc. Rev.* **2011**, *40*, 5361.
[46] Y. Yin, X. Li, S. Yan, H. Yan, C. Lu, *Chem. - Asian J.* **2018**, *13*, 3155.
[47] A. R. Davis, J. J. Peterson, K. R. Carter, *ACS Macro Lett.* **2012**, *1*, 469.
[48] S.-Y. Kim, J.-D. Lee, Y.-J. Cho, M. Rang Son, H.-J. Son, D. Won Cho, S. Ook Kang, *Phys. Chem. Chem. Phys.* **2018**, *20*, 17458.
[49] K. Kokado, Y. Chujo, *Macromolecules* **2009**, *42*, 1418.
[50] K.-R. Wee, Y.-J. Cho, J. K. Song, S. O. Kang, *Angew. Chem., Int. Ed.* **2013**, *52*, 9682.
[51] K. L. Martin, A. Krishnamurthy, J. Strahan, E. R. Young, K. R. Carter, *J. Phys. Chem. A* **2019**, *123*, 1701.
[52] J. H. Lee, H. Hwang, K. M. Lee, *J. Organomet. Chem.* **2016**, *825-826*, 69.
[53] H. J. Bae, H. Kim, K. M. Lee, T. Kim, Y. S. Lee, Y. Do, M. H. Lee, *Dalton Trans.* **2014**, *43*, 4978.
[54] J. J. Peterson, M. Werre, Y. C. Simon, E. B. Coughlin, K. R. Carter, *Macromolecules* **2009**, *42*, 8594.
[55] S. Inagi, K. Hosoi, T. Kubo, N. Shida, T. Fuchigami, *Electrochemistry* **2013**, *81*, 368.
[56] K. Kokado, A. Nagai, Y. Chujo, *Macromolecules* **2010**, *43*, 6463.
[57] K. Kokado, Y. Chujo, *Polym. J.* **2010**, *42*, 363.
[58] K. Kokado, Y. Chujo, *Dalton Trans.* **2011**, *40*, 1919.
[59] K. Kokado, Y. Chujo, *J. Org. Chem.* **2011**, *76*, 316.
[60] K. Kokado, A. Nagai, Y. Chujo, *Tetrahedron Lett.* **2011**, *52*, 293.
[61] M. Tominaga, H. Naito, Y. Morisaki, Y. Chujo, *Asian J. Org. Chem.* **2014**, *3*, 624.
[62] M. Tominaga, H. Naito, Y. Morisaki, Y. Chujo, *New J. Chem.* **2014**, *38*, 5686.
[63] Y.-J. Cho, S.-Y. Kim, M. Cho, W.-S. Han, H.-J. Son, D. Won Cho, S. Ook Kang, *Phys. Chem. Chem. Phys.* **2016**, *18*, 9702.
[64] Y.-C. Duan, Y. Gao, Y. Geng, Y. Wu, G.-G. Shan, L. Zhao, M. Zhang, Z.-M. Su, *J. Mater. Chem. C* **2019**, *7*, 2699.
[65] R. Furue, T. Nishimoto, I. S. Park, J. Lee, T. Yasuda, *Angew. Chem., Int. Ed.* **2016**, *55*, 7171.
[66] X. Li, Y. Yin, H. Yan, C. Lu, *Chem. - Asian J.* **2017**, *12*, 2207.
[67] D. K. You, J. H. Lee, B. H. Choi, H. Hwang, M. H. Lee, K. M. Lee, M. H. Park, *Eur. J. Inorg. Chem.* **2017**, *2017*, 2496.
[68] E. Berksun, I. Nar, A. Atsay, İ. Özçeşmeci, A. Gelir, E. Hamuryudan, *Inorg. Chem. Front.* **2018**, *5*, 200.
[69] K. Kokado, M. Tominaga, Y. Chujo, *Macromol. Rapid Commun.* **2010**, *31*, 1389.
[70] K. Tanaka, K. Nishino, S. Ito, H. Yamane, K. Suenaga, K. Hashimoto, Y. Chujo, *Faraday Discuss.* **2017**, *196*, 31.
[71] K. Kokado, Y. Tokoro, Y. Chujo, *Macromolecules* **2009**, *42*, 9238.
[72] H. Naito, K. Nishino, Y. Morisaki, K. Tanaka, Y. Chujo, *Chem. - Asian J.* **2017**, *12*, 2134.
[73] M. Tominaga, Y. Morisaki, H. Naito, Y. Chujo, *Polym. J.* **2014**, *46*, 740.
[74] Z. Wang, T. Wang, C. Zhang, M. G. Humphrey, *Phys. Chem. Chem. Phys.* **2017**, *19*, 12928.
[75] K. Kokado, Y. Tokoro, Y. Chujo, *Macromolecules* **2009**, *42*, 2925.
[76] M. Chaari, Z. Kelemen, J. Giner Planas, F. Teixidor, D. Choquesillo-Lazarte, A. B. Salah, C. Viñas, R. Núñez, *J. Mater. Chem. C* **2018**, *6*, 11336.
[77] D. Tu, P. Leong, Z. Li, R. Hu, C. Shi, K. Yin Zhang, H. Yan, Q. Zhao, *Chem. Commun.* **2016**, *52*, 12494.
[78] A. R. Cook, M. Valášek, A. M. Funston, P. Poliakov, J. Michl, J. R. Miller, *J. Phys. Chem. A* **2018**, *122*, 798.
[79] B. P. Dash, R. Satapathy, E. R. Gaillard, K. M. Norton, J. A. Maguire, N. Chug, N. S. Hosmane, *Inorg. Chem.* **2011**, *50*, 5485.
[80] W. N. Lipscomb, *Proc. Natl. Acad. Sci. USA* **1961**, *47*, 1791.
[81] T. L. Heying, J. W. Ager, S. L. Clark, D. J. Mangold, H. L. Goldstein, M. Hillman, R. J. Polak, J. W. Szymanski, *Inorg. Chem.* **1963**, *2*, 1089.
[82] U. Kusari, Y. Li, M. G. Bradley, L. G. Sneddon, *J. Am. Chem. Soc.* **2004**, *126*, 8662.
[83] U. Kusari, P. J. Carroll, L. G. Sneddon, *Inorg. Chem.* **2008**, *47*, 9203.
[84] Y. Li, P. J. Carroll, L. G. Sneddon, *Inorg. Chem.* **2008**, *47*, 9193.
[85] R. Coult, M. A. Fox, W. R. Gill, P. L. Herbertson, J. A. H. MacBride, K. Wade, *J. Organomet. Chem.* **1993**, *462*, 19.
[86] B. Stevens, M. I. Ban, *Trans. Faraday Soc.* **1964**, *60*, 1515.
[87] S. Sasaki, G. P. C. Drummen, G. Konishi, *J. Mater. Chem. C* **2016**, *4*, 2731.
[88] V. A. Galievsky, K. A. Zachariasse, *Acta Phys. Pol. A* **2007**, *112*, S.
[89] W. R. Dawson, M. W. Windsor, *J. Phys. Chem.* **1968**, *72*, 3251.
[90] M. Taniguchi, J. S. Lindsey, *Photochem. Photobiol.* **2018**, *94*, 290.
[91] G. E. Dobretsov, T. I. Syrejschikova, N. V. Smolina, *Biophysics* **2014**, *59*, 183.
[92] M. Sugino, Y. Araki, K. Hatanaka, I. Hisaki, M. Miyata, N. Tohnai, *Cryst. Growth Des.* **2013**, *13*, 4986.
[93] L. J. Farrugia, *J. Appl. Crystallogr.* **2012**, *45*, 849.